JPET Fast Forward. Published on May 3, 2010 as DOI: 10.1124/jpet.110.167544

JPET # 167544

# Inhibition or deletion of soluble epoxide hydrolase prevents hyperglycemia, promotes insulin secretion, and reduces islet apoptosis[*#]

**Pengcheng Luo, Hsin-Hsin Chang, Yiqiang Zhou, Shali Zhang, Sung Hee Hwang, Christophe Morisseau, Cong-Yi Wang, Edward W. Inscho, Bruce D. Hammock, and Mong-Heng Wang**

Department of Physiology (P.L., H.-H. C., Y.Z., S. Z., E.W.I., M.-H. W.), Medical College of Georgia, Augusta, GA 30912, USA.

Department of Nephrology (P.L.), Renmin Hospital of Wuhan University, Hubei Province 430060, P.R. China.

Department of Entomology and Cancer Center (S.H.H., C. M., B.D. H.), University of California, Davis, California.

Center for Biotechnology and Genomic Medicine (C.Y. W.), Department of Pathology, Medical College of Georgia, Augusta, GA30912, USA.

**a. Running title:** Soluble epoxide hydrolase in diabetes

**b. Send correspondence to:**

Mong-Heng Wang, Ph.D.

Department of Physiology

Medical College of Georgia

Augusta, GA 30912

Tel # 706-721-3830

Fax # 706-721-7299

Email: mwang@mail.mcg.edu

**c. Document statistics:**

Number of text pages: 29.
Number of Figures: 8.
Number of References: 34.
The number of words in the Abstract: 233.
The number of words in the Introduction: 511.
The number of words in the Discussion: 1475.

**d. Abbreviations:** $[Ca^{2+}]_i$, intracellular calcium concentration; CYP, cytochrome P450; DHET, dihydroxyeicosatrienoic acid; EET, epoxyeicosatrienoic acid; GSIS, glucose-stimulated insulin secretion; KO, knockout; NOD, nonobese diabetic; sEH, soluble epoxide hydrolase; STZ, streptozotocin; *t*-AUCB, *trans*-4-[4-(3-adamantan-1-ylureido)-cyclohexyloxy]-benzoic acid; UCP2, uncoupling protein 2.

JPET Fast Forward. Published on May 3, 2010 as DOI: 10.1124/jpet.110.167544
This article has not been copyedited and formatted. The final version may differ from this version.



**Abstract**

Soluble epoxide hydrolase (sEH) is an enzyme involved in the metabolism of endogenous inflammatory and anti-apoptotic mediators. However, the roles of sEH in diabetes and the pancreas are unknown. Our aims were to determine whether sEH is involved in the regulation of hyperglycemia in diabetic mice and to investigate the reasons for the regulation of insulin secretion by sEH deletion or inhibition in islets. We used two separate approaches, targeted disruption of *Ephx2* gene (sEH knockout (KO)) and a selective inhibitor of sEH (*t*-AUCB), to assess the role of sEH in glucose and insulin homeostasis in STZ mice. We also examined the effects of sEH KO or *t*-AUCB on glucose-stimulated insulin secretion (GSIS) and intracellular calcium levels in islets. Hyperglycemia in STZ mice was prevented by both sEH KO and *t*-AUCB. Also, STZ mice with sEH KO had improved glucose tolerance. Importantly, when insulin levels were assessed by hyperglycemic clamp study, sEH KO was found to promote insulin secretion. Also, sEH KO and *t*-AUCB treatment augmented islet GSIS. Islets with sEH KO had a greater intracellular calcium influx when challenged with high glucose or KCl in the presence of diazoxide. Moreover, sEH KO reduced islet cell apoptosis in STZ mice. These results demonstrate not only that sEH KO and its inhibition prevent hyperglycemia in diabetes, but that sEH KO enhances islet GSIS through the amplifying pathway and decreases islet cell apoptosis in diabetes.

## Introduction

The prevalence of diabetes continues to increase. It is estimated that 225 million people are affected worldwide (Mazzone, 2009). Moreover, diabetic population is subject to a high incidence of cardiovascular and renal diseases (Mazzone, 2009;Breyer et al., 2005). Diabetes is characterized by hyperglycemia related to abnormalities in the function of pancreatic β cells. Since β-cell destruction and dysfunction are the central events in the development and progression of diabetes, the prevention of β-cell destruction and the improvement of β-cell function could be important strategies for controlling the advance of diabetes (Kahn et al., 2006;Donath et al., 2008).

In pancreatic β cells, glucose stimulates insulin secretion by activating the triggering and amplifying pathways (Henquin, 2000). In the triggering pathway, products of glucose metabolism enter the mitochondrial respiratory chain, which uses them to generate adenosine triphosphate (ATP). Increased ATP levels close the $K_{ATP}$-sensitive channels, followed by membrane depolarization and opening of the voltage-sensitive $Ca^{2+}$ channels, which in turn increase intracellular $Ca^{2+}$ concentration and promote insulin secretion. In this pathway, uncoupling protein 2 (UCP2) acts as a negative regulator of glucose-stimulated insulin secretion (GSIS) by decreasing the production of ATP (Krauss et al., 2003). The amplifying pathway augments insulin release independently from its action on $K_{ATP}$-sensitive channels. The amplifying pathway can be studied by clamping $[Ca^{2+}]_i$ with high KCl in the presence of diazoxide, which holds $K_{ATP}$-sensitive channels open (Gembal et al., 1992).

JPET Fast Forward. Published on May 3, 2010 as DOI: 10.1124/jpet.110.167544
This article has not been copyedited and formatted. The final version may differ from this version.



It has been recognized that sEH, an enzyme, adds water to epoxide substrates, forming their corresponding 1,2-diol products. Extensive evidence has demonstrated that the protective effects of sEH inhibition are consequences of its ability to metabolize epoxyeicosatrienoic acids (EETs) (Chiamvimonvat et al., 2007). EETs, cytochrome P450 (CYP)-derived eicosanoids, have important biological properties in the kidneys and cardiovascular system (Imig, 2006;Roman, 2002). In the presence of NADPH and oxygen, arachidonic acid is metabolized by CYP epoxygenases into four EETs: 5,6-EET, 8,9-EET, 11,12-EET, and 14,15-EET. EETs are metabolized by sEH to the corresponding dihydroxyeicosatrienoic acids (DHETs) (Roman, 2002). In general, DHETs are much less biologically active than are EETs (Imig, 2005;Deng, et al., 2009). Therefore, inhibition of sEH activity has been used as a means of studying the biological functions of EETs (Imig, 2005;Imig, 2006).

Although it is well established that sEH inhibition has beneficial effects in cardiovascular and renal diseases (Chiamvimonvat, et al., 2007;Imig, 2005), the role of sEH in diabetes is still unknown. Several selective sEH inhibitors have been developed for long-term *in vivo* studies (Liu, et al., 2009). *Trans*-4-[4-(3-adamantan-1-ylureido)-cyclohexyloxy]-benzoic acid (*t*-AUCB) is a newly developed potent sEH inhibitor (Liu, et al., 2009) that has greater metabolic stability *in vivo* than do many sEH inhibitors (Liu, et al., 2009). In the present study, we investigated whether *t*-AUCB and sEH KO (*Ephx2* (-/-)) have any effects on the control of blood glucose homeostasis in streptozotocin (STZ)-treated mice. To control for any hemodynamic alternations, we also examined the role of sEH in β-cell function using isolated islets. To investigate whether sEH is involved in the prevention of β-cell loss, we also examined the effects of sEH KO on islet cell apoptosis in diabetes.

JPET Fast Forward. Published on May 3, 2010 as DOI: 10.1124/jpet.110.167544
This article has not been copyedited and formatted. The final version may differ from this version.



## Methods

### *Experimental Animal and Genotypic Analysis*

*Ephx2* (-/-) (B6.129X-*Ephx2*$^{tm1gonz}$/J) mice were obtained from Jackson Laboratory (Bar Harbor, ME). These mice were backcrossed with C57BL/6J mice for five generations to produce heterozygous *Ephx2* (+/-) offspring. The resulting *Ephx2* (+/-) offspring were intercrossed to generate *Ephx2* (+/+) and *Ephx2* (-/-) mice.

We obtained tail snips from litters at weaning (about 3 weeks of age). The DNA from tail snips was used to identify murine genotype by PCR. Routine genotyping of *Ephx2* (+/+), *Ephx2* (+/-), and *Ephx2* (-/-) mice was done using the following primers: F1, 5'-CTTGGCAGGGTTTCTAGTCCTTAG-3'; R1, 5'-CACGCTGGCATTTTAACACCAG-3'; F2, 5'-CGCTTCCTCGTGCTTTACGGTATC-3'; and R2, GTCAAGGTCGAACGCGGCTACAC-3'. Primer F1/R1 predicts a 510-base pair amplicon for the wild-type allele. For the *Ephx2* null allele, primer F2/R2 predicts a 160-base pair product of a neomycin-resistance sequence as described previously (Sinal, et al., 2000). These primers were designed by Lasergene 7 software (DNAstar, Madison, WI). The genotypic analysis was examined using 3% Nusieve GTG agarose gel (Lonza, Rockland, ME). All animal protocols were approved by the Institutional Animal Care and Use Committee and were in accord with the requirements stated in the National Institute of Health *Guide for the Care and Use of Laboratory Animals*.

### *Western Blot Analysis*

Expression of sEH, UCP2, and β-actin was analyzed by homogenization of tissues or cells. Samples from *Ephx2* (+/+) and *Ephx2* (-/-) mice, as well as NIT-1 cells, were separated by electrophoresis for 3 h. The proteins were transferred to an enhanced chemiluminescence (ECL) membrane in a transfer buffer. The membranes were blocked for 90 min with 5% nonfat dry

milk in Tris-buffered saline. The membranes were incubated with antibody against human sEH (1:1000), against mouse UCP2 (1:500; Alpha Diagnostic, San Antonio, TX), or against β-actin (1:5000; Sigma, St. Louis, MO). The membranes were incubated with secondary antibody for sEH, UCP2, or β-actin. Chemiluminescent detection using ECL reagent from Amersham Biosciences (Piscataway, NJ) was done on X-ray film. In addition, quantification of sEH levels in mouse islets was done with the Odyssey® infrared imaging system and analyzed with NIH image J software.

***STZ-Induced Diabetes and the Treatment of t-AUCB***

Diabetes was induced in *Ephx2* (+/+) and *Ephx2* (-/-) mice by injection of STZ as previously described (Yoon, et al., 2001). We treated 6-week-old male *Epxh2* (+/+) mice with STZ (50 mg/kg/day for 3 days, i.p.), STZ plus *t*-AUCB (10 mg/l in drinking water), or vehicle. We also treated age-matched *Ephx2* (-/-) mice with the same dose of STZ or vehicle.

***Blood Glucose, Plasma Insulin, and Plasma Glucagon***

Blood glucose concentrations were measured with a glucometer (Accu-Check blood glucose monitor system, Roche Diagnostics, Indianapolis, IN). Plasma insulin concentrations were measured using mouse insulin as a standard (rat insulin ELISA kit, Crystal Chemical, Chicago, IL). Plasma glucagon concentrations were measured using a glucagon ELISA kit (Cosmo Bio, Tokyo, Japan).

***Hyperglycemic Clamp and Glucose Tolerance Studies***

Hyperglycemic clamp study was done using continuous infusion of glucose from the jugular vein in a modified version of a previously published method (Danial, et al., 2008). Male *Ephx2* (-/-) and *Ephx2* (+/+) mice aged 12 to 18 weeks were cannulated with tubing (OD 0.64

mm, Silastic, Mildland, MI) into the right internal jugular vein for continuous infusion of glucose. After 2~3 days of recovery from surgery, clamp analysis was done on 6-h fasted and conscious mice. Variable infusion of a 20% glucose solution was started at time 0 and periodically adjusted to sequentially clamp plasma glucose concentrations at about 450 mg/dl. Blood samples were collected from mouse tails at 5-10 min intervals for 120 min for use in the measurement of plasma insulin by an ELISA kit (Linco Research, St. Charles, MO). Intraperitoneal glucose tolerance tests (IGTT) were performed on 12-16-week-old mice. STZ mice were fasted for 6 h and injected i.p. with glucose (1 g/kg body weight). Blood glucose concentrations were determined with a glucometer at 0, 10, 30, 60, and 120 min after glucose administration (Uysal, et al., 1997). Plasma insulin concentrations were determined by an ELISA kit at 0, 30, 60, and 120 min after glucose administration. The values of area under the curve for blood glucose ($AUC_{glucose}$) and insulin ($AUC_{insulin}$) in IGTT were determined by GraphPad software (La Jolla, CA). Insulin tolerance tests were performed similarly by injecting human insulin (1 U/kg body weight). Glucose concentrations were measured at 0, 10, 30, and 60 min after insulin administration.

***Pancreatic Islet Isolation, Insulin Secretion, Islet ATP Concentrations, and Islet Cell Apoptosis***

Pancreatic islets were isolated by a modified collagenase digestion method as previously described (Oshima, et al., 2006;Zhang, et al., 2001). Anesthetized *Ephx2* (-/-) and *Ephx2* (+/+) mice were sacrificed by cervical dislocation. The common duct was clamped at its entrance to the duodenum and cannulated under a dissecting microscope. Pancreatic inflation was accomplished via the bile duct with 2.0-2.5 ml of 0.5 mg/ml collagenase XI (Roche, Indianapolis, IN) dissolved in Hank's buffer supplemented with 1 mM $MgCl_2$ and 10 mM HEPEs. The distended pancreases were removed and incubated with type XI collagenase

JPET Fast Forward. Published on May 3, 2010 as DOI: 10.1124/jpet.110.167544
This article has not been copyedited and formatted. The final version may differ from this version.



(Roche, Indianapolis, IN) in glass vials for about 17 min at 37°C. During the incubation, we manually agitated the glass vials containing pancreases to achieve tissue disintegration. The islets were hand-picked three to four times under a dissecting microscope; we estimated that we obtained about 80-100 islets per mouse. We then cultured islets overnight in DME medium containing 8.3 mM glucose and supplemented with 1% penicillin-streptomycin, 7.5% fetal bovine serum and 10 mM HEPEs at 37°C. Islets were pooled and washed 3 times with Krebs buffer (in mM, 119 NaCl, 4.6 KCl, 1 $MgSO_4$, 0.15 $Na_2HPO_4$, 0.4 $KH_2PO_4$, 25 $NaHCO_3$, 2 $CaCl_2$, 20 HEPEs at pH 7.4 and 0.05%, wt/vol, BSA). The islets (5 islets per sample) were then incubated in Krebs buffer containing 3 mM glucose for 1 h at 37°C and pelleted (800g for 5 min), after which their medium was aspirated and replaced for 1 h with 1.0 ml Krebs solution containing different concentrations of glucose or 30 mM KCl plus 250 μM diazoxide plus 3 mM glucose. KCl solutions were prepared by equalmolar substitution of NaCl to maintain iso-osmolarity. Five parallel repeats were done for each condition. Islet ATP concentrations were determined by a luciferase-based assay on 50 islets per tube as previously described (Krauss, et al., 2003). For *in vitro* sEH inhibition experiments, *Ephx2* (+/+) islets were treated in the same manner except that DME medium and Krebs buffer containing 100 μM *t*-AUCB dissolved in DMSO were used. All pellets were solubilized to assess intracellular insulin content. The supernatant and pellets were collected and assayed for insulin using an ELISA kit (Linco Research). Insulin release data were determined by the ratio of insulin levels in supernatant to insulin levels in pellets. To determine islet apoptosis, mouse pancreases isolated from *Ephx2* (-/-) and *Ephx2* (+/+) mice given different treatments were fixed, sectioned, and TUNEL stained. The TUNEL assay was done using the ApopTag Plus Peroxidase In Situ Apoptosis Detection Kit (Millipore, Temecula, CA) according to the manufacturer's instructions. Apoptosis was scored as the average number of TUNEL-positive cells per 100 islet cells. The data were expressed as the relative fold change of TUNEL-positive cells per 100 islet cells in the STZ-*Ephx2* (+/+)

JPET Fast Forward. Published on May 3, 2010 as DOI: 10.1124/jpet.110.167544
This article has not been copyedited and formatted. The final version may differ from this version.



group compared with the STZ-*Ephx2* (-/-) group (Dai, et al., 2009).

***Intracellular Calcium Concentration Measurement in Islet Cells***

Fluorescence experiments were performed using monochromator-based fluorescence spectrophotometry (Photon Technology International, London, Ontario, Canada) as previously described (Inscho, et al., 1999). Excitation wavelengths were set at 340 and 380 nm; emitted light was collected at 510 ± 20 nm. Fluorescence intensity was collected at 10 data points/sec. These data were analyzed using FeliX software (Photon Technology International).

Islets were dissociated into single cells by incubation in trypsin at 37°C for 10 min, then washed twice before being allowed to attach to glass coverslips. Cells were incubated overnight in RPMI 1640 medium with 10% FBS and 1% penicillin-streptomycin. Cells were transferred to a fura 2 loading solution containing 5 μM fura 2 acetoxymethyl ester (fura 2-AM; Molecular Probes, Eugene, OR) in serum-free DMEM for 30-45 min at 37°C. Coverslips of fura 2-loaded cells were mounted in a perfusion chamber (Warner Instrument, Hamden, CT) and affixed to the stage of an Olympus® IX50 inverted light microscope. The cells were continuously superfused (1.4 ml/min; 25°C) with normal $Ca^{2+}$ solution (in mM, 120 NaCl, 5 KCl, 25 $NaHCO_3$, 2.5 $CaCl_2$, 1.1 $MgCl_2$, 25 HEPEs, titrated to pH 7.4) containing 3 mM glucose, then challenged with 25 mM glucose or 30 mM KCl plus 250 μM diazoxide plus 3 mM glucose. High $K^+$ solutions were prepared by equimolar substitutions of KCl for NaCl. Fluorescence data were collected with background subtraction.

***Statistical Analysis***

All values are expressed as means ± SE. All data were analyzed by SPSS computer software (SPSS, Chicago, IL). We used one-way ANOVA and Student-Neuman-Keuls tests for

JPET Fast Forward. Published on May 3, 2010 as DOI: 10.1124/jpet.110.167544
This article has not been copyedited and formatted. The final version may differ from this version.



multiple comparisons or Independent Student's *t* test for unpaired groups. Statistical significance was set at $P < 0.05$ or 0.01.

## Results

### *Genotyping for Ephx2 (-/-), Ephx2 (+/-), and Ephx2 (+/+) Mice*

Heterozygous *Ephx2* (+/-) mice were interbred to generate homozygous *Ephx2* (-/-) mice and their littermate controls, *Ephx2* (+/+) mice. The genotypes of *Ephx2* (-/-), *Ephx2* (+/-), and *Ephx2* (+/+) mice are shown in Fig. 1A. To confirm that sEH protein is deleted in *Ephx2* (-/-) mice, Western blot analysis was done on tissues isolated from *Ephx2* (+/+) and *Ephx2* (-/-) mice. As shown in Fig. 1B, sEH protein was expressed in different tissues of *Ephx2* (+/+) mice, but was absent in *Ephx2* (-/-) mice. In addition, we estimated that the concentration of sEH in mouse islets is about 0.93 ng/μg protein (Fig. 1C). To determine whether sEH is expressed in β-cells, we did Western blot of sEH in NIT-1 cells (nonobese diabetic (NOD) mouse–derived β-cell line). We found that sEH is expressed in these cells (Fig. 1D), suggesting that sEH is expressed in β cells.

### *sEH Knockout and Inhibition Prevent Hyperglycemia in STZ-Diabetic Mice*

To investigate the effect of sEH KO on glucose homeostasis in diabetes, we induced diabetes in *Ephx2* (-/-) and *Ephx2* (+/+) mice by injecting them with a low dose of STZ (50 mg/kg/day of STZ for 3 days, i.p.). To determine whether sEH inhibition has effects similar to those of sEH KO, we simultaneously treated *Ephx2* (+/+) mice with STZ and *t*-AUCB. *Ephx2* (+/+) mice treated with STZ had elevated blood glucose. *t*-AUCB treatment prevented hyperglycemia in *Ephx2* (+/+) mice treated with STZ (Fig. 2). Interestingly, blood glucose levels in STZ-treated *Ephx2* (-/-) mice were only slightly elevated (Fig. 2). In addition, we found no difference in the average blood glucose values of *Ephx2* (+/+) and *Ephx2* (-/-) mice injected with vehicle. These intriguing results provide convincing evidence that sEH deletion and its

inhibition prevent hyperglycemia in STZ-induced diabetes.

***sEH Knockout Causes Higher Plasma Insulin Levels***

To determine the effects of sEH KO on glucose and insulin homeostasis, we did IGTT on STZ-*Ephx2* (-/-) and STZ-*Ephx2* (+/+) mice. $AUC_{glucose}$ in STZ-*Ephx2* (-/-) mice was significantly lower than that in STZ-*Ephx2* (+/+) mice (48360 ± 2468 vs. 63855 ± 3254 mg/dl x 120 min, n = 4, $P < 0.05$) (Fig. 3A). These results demonstrate that STZ-*Ephx2* (-/-) mice have significantly greater glucose tolerance than do STZ-*Ephx2* (+/+) mice. In contrast, $AUC_{insulin}$ in STZ-*Ephx2* (-/-) mice was significantly higher than that in STZ-*Ephx2* (+/+) mice (45 ± 2.6 vs. 30 ± 4.3 ng/ml x 120 min, n = 4, $P < 0.05$). It appears that the reason for increasing $AUC_{insulin}$ in STZ-*Ephx2* (-/-) mice is because STZ-*Ephx2* (-/-) mice have higher basal insulin levels than STZ-*Ephx2* (+/+) mice (Fig. 3B).

To determine the effect of sEH on *in vivo* insulin secretion, we used hyperglycemic clamp study to assess insulin secretion in *Ephx2* (-/-) and *Ephx2* (+/+) mice (Fig. 4A). Fasting *Ephx2* (-/-) and *Ephx2* (+/+) mice were infused with intravenous glucose as needed to maintain blood glucose levels at ~450 mg/dl in both groups. Notably, *Ephx2* (-/-) mice required a considerably higher glucose infusion rate than did *Ephx2* (+/+) mice to maintain this blood glucose concentration (Fig. 4B). Moreover, the insulin secretion response in *Ephx2* (-/-) mice during hyperglycemia was significantly higher than that in *Ephx2* (+/+) mice (Fig. 4C), providing important evidence that sEH KO increases GSIS *in vivo*. Insulin tolerance tests demonstrated that insulin sensitivity was equal in *Ephx2* (+/+) and *Ephx2* (-/-) mice (Fig. 5A). To evaluate whether glucagon is involved in the regulation of blood glucose concentrations in *Ephx2* (-/-) mice, we determined fed and fasted plasma glucagon levels in *Ephx2* (-/-) and *Ephx2* (+/+) mice, finding they were similar (Fig. 5B).

JPET Fast Forward. Published on May 3, 2010 as DOI: 10.1124/jpet.110.167544
This article has not been copyedited and formatted. The final version may differ from this version.



***sEH Knockout and Inhibition Increase Insulin Secretion in Islets***

Since both *Ephx2* gene deletion and pharmacological inhibitors suppress sEH activity throughout the body, it is hard to determine whether the effects of sEH deletion and inhibition are pancreas-specific or reflect whole-body actions. Also, hemodynamic effects due to sEH inhibition or deficiency may cause altered insulin secretion. To evaluate the direct effects of sEH KO on insulin secretion and to determine whether this enhanced insulin secretion is also manifested *in vitro*, islets harvested from *Ephx2* (+/+) and *Ephx2* (-/-) mice were challenged with 3 mM glucose, 25 mM glucose, or 30 mM KCl plus 250 μM diazoxide plus 3 mM glucose. *Ephx2* (-/-) and *Ephx2* (+/+) islets incubated with 3 mM glucose secreted similar amounts of insulin. However, when islets were challenged with 25 mM glucose, *Ephx2* (-/-) islets secreted significantly greater amounts of insulin than did *Ephx2* (+/+) islets. Insulin secretion stimulated by KCl plus diazoxide plus 3 mM glucose was significantly higher in *Ephx2* (-/-) islets than in *Ephx2* (+/+) islets (Fig. 6A). We also incubated *Ephx2* (+/+) islets with or without *t*-AUCB (100 μM) and challenged them with 25 mM glucose. Under these conditions, *Ephx2* (+/+) islets incubated with *t*-AUCB secreted significantly higher amounts of insulin than did vehicle-treated islets (Fig. 6B). Similarly, insulin secretion by *Ephx2* (+/+) islets incubated with *t*-AUCB and stimulated with KCl plus diazoxide plus 3 mM glucose was significantly higher than that in the absence of *t*-AUCB incubation (Fig. 6B). To determine whether sEH KO has any effect on ATP levels, *Ephx2* (-/-) and *Ephx2* (+/+) islets were incubated with varying concentrations of glucose. sEH KO did not affect ATP concentrations in islets incubated with either 3 mM or 25 mM glucose (Fig. 6C). To assess whether sEH KO has any effect on UCP2, we determined the expression levels of UCP2 by Western blot in *Ephx2* (-/-) and *Ephx2* (+/+) islets, finding that sEH KO did not affect expression levels of UCP2 (Fig. 6D).

***sEH Knockout Increases $[Ca^{2+}]_i$ Response to High Glucose and KCl Plus Diazoxide***

To determine whether sEH KO affects $[Ca^{2+}]_i$ in response to different stimulators, we monitored changes in $[Ca^{2+}]_i$ in *Ephx2* (-/-) and *Ephx2* (+/+) islet cells exposed to 3 mM glucose, 25 mM glucose, or 30 mM KCl plus 250 μM diazoxide plus 3 mM glucose. Basal $[Ca^{2+}]_i$ levels were similar at 3 mM glucose in *Ephx2* (-/-) and *Ephx2* (+/+) islet cells, suggesting that sEH KO does not affect the basic control mechanism of $Ca^{2+}$ handling. Compared with 3 mM glucose, $[Ca^{2+}]_i$ increased rapidly in response to 25 mM glucose in both *Ephx2* (-/-) and *Ephx2* (+/+) islet cells. However, *Ephx2* (-/-) cells exhibited higher $[Ca^{2+}]_i$ levels than did *Ephx2* (+/+) cells (Figs. 7A, B); these results paralleled those for insulin secretion in islets (Fig. 6A). Similarly, the effects of KCl plus diazoxide plus 3 mM glucose on $[Ca^{2+}]_i$ were significantly greater in *Ephx2* (-/-) cells than in *Ephx2* (+/+) cells (Fig. 7).

***sEH Knockout Reduces Islet Cell Apoptosis in STZ Mice***

It is well established that immune-cell secreted proinflammatory cytokines are important in the pathogenesis of STZ-induced diabetes (Fukuda, et al., 2008;Muller, et al., 2002). These proinflammatory cytokines promote islet cell apoptosis and result in hyperglycemia. To determine whether sEH KO has any effects on apoptosis, 6-week-old male *Ephx2* (+/+) and *Ephx2* (-/-) mice were given either STZ (50 mg/kg/day for 3 days, i.p.) or vehicle. On day 14 after the initial STZ treatment, we examined islet cell apoptosis. As shown in Fig. 8A, we did not observe any apoptosis in pancreatic sections of *Ephx2* (+/+) or *Ephx2* (-/-) mice treated with vehicle. STZ treatment induced significant islet cell apoptosis in *Ephx2* (+/+) mice, but a marked reduction in islet cell apoptosis was observed in *Ephx2* (-/-) mice (Fig. 8).

**Discussion**

Since pancreatic β-cell loss and dysfunction are central factors in the pathogenesis of diabetes, preventing β-cell loss and diminishing β-cell dysfunction are potentially useful approaches to enhancing glucose homeostasis in diabetes (Henquin, 2004). Although it is well established that the inhibition of sEH lowers blood pressure in various animal models (Loch, et al., 2007;Imig, et al., 2002;Imig, 2005), the involvement of sEH in the control of blood glucose in diabetes is unknown. Here, for the first time, we demonstrate that sEH has a role in glucose homeostasis, insulin secretion, and islet cell apoptosis.

Since insulin is the major hormone that lowers blood glucose levels, we hypothesized that sEH has a critical function in regulating insulin homeostasis and examined the effect of sEH KO on glucose homeostasis in STZ mice. Glucose tolerance tests of STZ mice showed that sEH KO improved glucose tolerance and increased plasma insulin concentrations (Figs. 3A and 3B). These results suggest that preventing hyperglycemia by sEH KO in diabetic mice is probably due to increased GSIS in pancreatic β cells. To test this possibility, we did hyperglycemic clamp study of *Ephx2* (-/-) and *Ephx2* (+/+) mice, finding that sEH KO significantly enhanced insulin secretion (Fig. 4C). Since insulin sensitivity is equal in *Ephx2* (+/+) and *Ephx2* (-/-) mice (Fig. 5A), these results demonstrate that *Ephx2* (-/-) mice release more insulin than do *Ephx 2* (+/+) mice without changing their insulin sensitivity.

Insulin is secreted by pancreatic β cells in response to high glucose, whereas glucagon is secreted by pancreatic α cells during hypoglycemia. Under normal physiological conditions, elevated glucose or insulin levels inhibit glucagon release from α cells (Gromada, et al., 2009). Insulin promotes glucose uptake from peripheral tissues and stimulates the synthesis of glycogen

and lipids, whereas glucagon opposes the actions of insulin (Gromada, et al., 2009). Thus, the balance between these two hormones holds blood glucose levels within a narrow physiological range. To determine whether sEH KO affects circulating levels of glucagon, we measured fed and fasted plasma glucagon concentrations in *Ephx2* (-/-) and *Ephx2* (+/+) mice. We found that these mice had comparable levels of plasma glucagon (Fig. 5B), indicating that the effects of sEH KO on glucose homeostasis are due to insulin rather than glucagon.

Since sEH KO promotes insulin secretion *in vivo*, we determined whether sEH is significantly expressed in islets and β cells. Using purified sEH, we estimated that the concentration of sEH in mouse islets is about 0.93 ng/μg protein (Fig. 1C). Thus, a significant amount of sEH is expressed in islets. To determine whether sEH is expressed in β cells, we used an immunohistochemical method in an attempt to determine the expression of sEH in pancreatic cells. We tried two sources of antibodies, Dr. B.D. Hammock and Santa Cruz Biotechnology (Santa Cruz, CA). However, these antibodies were not suitable for immunohistochemical analysis (data not shown). Alternatively, we did Western blot analysis of sEH in NIT-1 cells (NOD-derived β-cell line), finding that sEH is expressed in NIT-1 cells (Fig. 1D). This suggests that sEH is expressed in β cells.

To investigate the mechanism for the stimulation of insulin release by sEH KO in glucose homeostasis, we assessed whether sEH KO and inhibition affect islet GSIS. We found that both sEH KO and inhibition significantly stimulated islet GSIS, suggesting that deletion and inhibition of sEH are involved in enhancing GSIS in pancreatic β cells. It is well established that the $K_{ATP}$-channel-dependent pathway is essential in the stimulation of insulin secretion by glucose and has the vital function of triggering the pathway for GSIS in β cells (Chan, et al.,

JPET Fast Forward. Published on May 3, 2010 as DOI: 10.1124/jpet.110.167544
This article has not been copyedited and formatted. The final version may differ from this version.



2004;Gupta, et al., 2005;Henquin, 2009). In the $K_{ATP}$-channel-dependent pathway for insulin release occurs as follows, glucose is oxidized in β cells to generate NADH and $FADH_2$, which donate electrons to the electron transport chain located in the mitochondrial matrix to create a proton electrochemical gradient; protons then reenter the mitochondrial matrix to generate ATP; increased ATP closes the $K_{ATP}$ channel, causing membrane depolarization, increasing the cytoplasmic calcium concentration and consequently activating insulin secretion through calcium-dependent exocytosis (Gupta, et al., 2005;Zhang, et al., 2001;Kahn, et al., 2006;Zhang, et al., 2001). Since ATP and UCP2 are the key components of this pathway, we next determined whether sEH KO affects ATP content and UCP2 levels in islets. We found no difference between *Ephx2* (-/-) and *Ephx2* (+/+) islets with response to ATP content (Fig. 6C) or UCP2 expression (Fig. 6D), suggesting that the mechanism that stimulates insulin release by sEH KO probably is not mediated through the $K_{ATP}$-channel-dependent pathway.

It is widely accepted that any pharmacological agents interfering with elevation of intracellular calcium concentration ($[Ca^{2+}]_i$) in β cells causes impairment of GSIS, whereas any agents that increase $[Ca^{2+}]_i$ promote insulin release in β cells (Henquin, 2009). Thus, $[Ca^{2+}]_i$ serves as a triggering signal for insulin release in β cells (Henquin, 2000). To examine whether sEH KO affects $[Ca^{2+}]_i$ in response to different stimulators, we did calcium-photometry analysis in cultured *Ephx2* (-/-) and *Ephx2* (+/+) islet cells. We found that $[Ca^{2+}]_i$ increased more rapidly in *Ephx2* (-/-) islet cells than it did in *Ephx2* (+/+) islet cells in response to both high glucose and high KCl plus diazoxide, an approach used to evaluate the amplifying pathway (Henquin, 2000) (Fig. 7). These findings indicate that the effects of sEH KO on the enhancement of islet GSIS are mediated through the amplifying pathway. However, the molecular mechanisms whereby sEH KO enhances islet GSIS through this pathway require further investigation.

The present study provides new information about the prevention of hyperglycemia by sEH KO and inhibition in diabetes, as well as the beneficial effect of sEH KO and inhibition on islet GSIS. Nevertheless, the exact mechanisms by which sEH KO or inhibition prevents hyperglycemia and influences insulin secretion are still not known.

The possible reasons for the effects of sEH KO or inhibition *in vitro* and *in vivo* may be explained as follow. Although the promotion of islet GSIS by sEH KO is an important reason for the prevention of hyperglycemia in STZ mice, other biological activity derived from sEH KO can contribute to this beneficial effect. Abundant evidence indicates that immune-cell-secreted proinflammatory cytokines are important in the pathogenesis of STZ-induced diabetes (Fukuda, et al., 2008;Muller, et al., 2002). Since proinflammatory cytokines are also important in the causation of β-cell apoptosis, we hypothesize that the prevention of hyperglycemia by sEH KO is due to its anti-apoptotic property. To test this hypothesis, we determined whether sEH KO affects islet cell apoptosis in STZ model, finding that STZ-*Ephx2* (-/-) mice exhibited lower islet cell apoptosis than did STZ-*Ephx2* (+/+) mice (Fig. 8). Interestingly, Simpkin *et al.* have recently demonstrated that the inhibition of sEH by AUDA decreases the expression of proapoptotic genes in neural tissues (Simpkins, et al., 2009). Taken together, these results demonstrate that anti-apoptotic property of sEH KO in islets is an important mechanism in preventing hyperglycemia in diabetes.

It is well accepted that sEH KO and inhibition increase EETs level by decreasing the degradation of EETs (Chiamvimonvat, et al., 2007). In accord with this, Liu *et al.* (Liu, et al., 2009) have demonstrated that *t*-AUCB treatment reduces the production of DHETs and increases the ratios of EETs to DHETs in the plasma of LPS-treated mice. Similarly, Seubert *et*

*al*. (Seubert, et al., 2006) reported that *Ephx2* (-/-) mice have higher plasma ratios of EETs to DHETs than do wild-type mice. Thus, it is likely that sEH KO or inhibition by *t*-AUCB causes elevation of pancreatic EETs level and contributes to the enhancement of GSIS. In this regard, Zeldin and colleagues (Zeldin, et al., 1997) reported that CYP2J protein is expressed in human and rat pancreatic tissues and noted that significant amounts of endogenous EETs are present in the human and rat pancreas. Falck *et al.* (Falck, et al., 1983) have shown that EETs are potent mediators of insulin release in isolated rat islets. Nevertheless, it remains unclear which CYP isoforms are responsible for the generation of EETs in the mouse pancreas and whether EETs are able to promote insulin release in mouse islets.

In summary, we have made the novel findings that sEH KO and inhibition prevent hyperglycemia of STZ-diabetic mice. Our hyperglycemic clamp experiments support the possibility that the prevention of hyperglycemia by sEH KO is caused by increased insulin secretion from β cells. Our *in vitro* findings demonstrate that sEH KO and its inhibition increase GSIS by islets. It appears that the enhancement of GSIS by sEH KO in β cells is mediated through the amplifying pathway and sEH KO reduces islet apoptosis during diabetes. Since both sEH KO and sEH inhibitor prevent the elevation of blood glucose levels in diabetic animals, this study raises the possibility that, in addition to their anti-hypertensive and anti-inflammatory effects, sEH KO and inhibitors may be promising approaches to the prevention of hyperglycemia in diabetes mellitus.

**Acknowledgement**

We thank Dr. Philippe A. Halban of the Department of Genetic Medicine and Development, University of Geneva, Switzerland for instructions on islet isolation; Dr. James Matthew Luther, Division of Clinical Pharmacology, Vanderbilt University for instructions on the hyperglycemic clamp study; and Dr. Michael Brands, Medical College of Georgia, for the discussion during the preparation of this manuscript.

## References

Breyer MD, Bottinger E, Brosius FC, III, Coffman TM, Harris RC, Heilig CW and Sharma K (2005) Mouse models of diabetic nephropathy. *J Am Soc Nephrol* **16**:27-45.

Chan CB, Saleh MC, Koshkin V and Wheeler MB (2004) Uncoupling protein 2 and islet function. *Diabetes* **53**:S136-S142.

Chiamvimonvat N, Ho CM, Tsai HJ and Hammock BD (2007) The soluble epoxide hydrolase as a pharmaceutical target for hypertension. *J Cardiovasc Pharmacol* **50**:225-237.

Dai T, Patel-Chamberlin M, Natarajan R, Todorov I, Ma J, LaPage J, Phillips L, Nast CC, Becerra D, Chuang P, Tong L, de BJ, Wells DJ, Wang Y and Adler SG (2009) Heat shock protein 27 overexpression mitigates cytokine-induced islet apoptosis and streptozotocin-induced diabetes. *Endocrinology* **150**:3031-3039.

Danial NN, Walensky LD, Zhang CY, Choi CS, Fisher JK, Molina AJ, Datta SR, Pitter KL, Bird GH, Wikstrom JD, Deeney JT, Robertson K, Morash J, Kulkarni A, Neschen S, Kim S, Greenberg ME, Corkey BE, Shirihai OS, Shulman GI, Lowell BB and Korsmeyer SJ (2008) Dual role of proapoptotic BAD in insulin secretion and beta cell survival. *Nat Med* **14**:144-153.

Deng Y, Theken KN and Lee CR (2009) Cytochrome P450 epoxygenases, soluble epoxide hydrolase, and the regulation of cardiovascular inflammation. *J Mol Cell Cardiol* **48**:331-341.

Donath MY, Storling J, Berchtold LA, Billestrup N and Mandrup-Poulsen T (2008) Cytokines and beta-cell biology: from concept to clinical translation. *Endocr Rev* **29**:334-350.

Falck JR, Manna S, Moltz J, Chacos N and Capdevila J (1983) Epoxyeicosatrienoic acids stimulate glucagon and insulin release from isolated rat pancreatic islets. *Biochem Biophys Res Commun* **114**:743-749.

Fukuda K, Tesch GH, Yap FY, Forbes JM, Flavell RA, Davis RJ and Nikolic-Paterson DJ (2008) MKK3 signalling plays an essential role in leukocyte-mediated pancreatic injury in the multiple low-dose streptozotocin model. *Lab Invest* **88**:398-407.

Gembal M, Gilon P and Henquin JC (1992) Evidence that glucose can control insulin release independently from its action on ATP-sensitive $K^+$ channels in mouse B cells. *J Clin Invest* **89**:1288-1295.

Gromada J, Duttaroy A and Rorsman P (2009) The insulin receptor talks to glucagon? *Cell Metab* **9**:303-305.

Gupta RK, Vatamaniuk MZ, Lee CS, Flaschen RC, Fulmer JT, Matschinsky FM, Duncan SA and Kaestner KH (2005) The MODY1 gene HNF-4alpha regulates selected genes involved in insulin secretion. *J Clin Invest* **115**:1006-1015.

Henquin JC (2000) Triggering and amplifying pathways of regulation of insulin secretion by glucose. *Diabetes* **49**:1751-1760.

Henquin JC (2004) Pathways in beta-cell stimulus-secretion coupling as targets for therapeutic insulin secretagogues. *Diabetes* **53**:S48-S58.

Henquin JC (2009) Regulation of insulin secretion: a matter of phase control and amplitude modulation. *Diabetologia* **52**:739-751.

Imig JD, Zhao X, Capdevila JH, Morisseau C and Hammock BD (2002) Soluble epoxide hydrolase inhibition lowers arterial blood pressure in angiotensin II hypertension. *Hypertension* **39**:690-694.

Imig JD (2005) Epoxide hydrolase and epoxygenase metabolites as therapeutic targets for renal diseases. *Am J Physiol* **289**:F496-F503.

Imig JD (2006) Cardiovascular therapeutic aspects of soluble epoxide hydrolase inhibitors. *Cardiovasc Drug Rev* **24**:169-188.

Inscho EW, LeBlanc EA, Pham BT, White SM and Imig JD (1999) Purinoceptor-mediated calcium signaling in preglomerular smooth muscle cells. *Hypertension* **33**:195-200.

Kahn SE, Hull RL and Utzschneider KM (2006) Mechanisms linking obesity to insulin resistance and type 2 diabetes. *Nature* **444**:840-846.

Krauss S, Zhang CY, Scorrano L, Dalgaard LT, St-Pierre J, Grey ST and Lowell BB (2003) Superoxide-mediated activation of uncoupling protein 2 causes pancreatic beta cell dysfunction. *J Clin Invest* **112**:1831-1842.

Liu JY, Tsai HJ, Hwang SH, Jones PD, Morisseau C and Hammock BD (2009) Pharmacokinetic optimization of four soluble epoxide hydrolase inhibitors for use in a murine model of inflammation. *Br J Pharmacol* **156**:284-296.

Loch D, Hoey A, Morisseau C, Hammock BO and Brown L (2007) Prevention of Hypertension in DOCA-Salt Rats by an Inhibitor of Soluble Epoxide Hydrolase. *Cell Biochem Biophys* **47**:87-98.

Mazzone T (2009) Hyperglycaemia and coronary heart disease: the meta picture. *Lancet* **373**:1737-1738.

Muller A, Schott-Ohly P, Dohle C and Gleichmann H (2002) Differential regulation of Th1-type and Th2-type cytokine profiles in pancreatic islets of C57BL/6 and BALB/c mice by multiple low doses of streptozotocin. *Immunobiology* **205**:35-50.

Oshima H, Taketo MM and Oshima M (2006) Destruction of pancreatic beta-cells by transgenic induction of prostaglandin E2 in the islets. *J Biol Chem* **281**:29330-29336.

Roman RJ (2002) P450 metabolites of arachidonic acid in the control of cardiovascular function. *Physiol Rev* **82**:131-185.

Seubert JM, Sinal CJ, Graves J, DeGraff LM, Bradbury JA, Lee CR, Goralski K, Carey MA, Luria A, Newman JW, Hammock BD, Falck JR, Roberts H, Rockman HA, Murphy E and Zeldin DC (2006) Role of soluble epoxide hydrolase in postischemic recovery of heart contractile function. *Circ Res* **99**:442-450.

Simpkins AN, Rudic RD, Schreihofer DA, Roy S, Manhiani M, Tsai HJ, Hammock BD and Imig JD (2009) Soluble epoxide inhibition is protective against cerebral ischemia via vascular and neural protection. *Am J Pathol* **174**:2086-2095.

Sinal CJ, Miyata M, Tohkin M, Nagata K, Bend JR and Gonzalez FJ (2000) Targeted disruption of soluble epoxide hydrolase reveals a role in blood pressure regulation. *J Biol Chem* **275**:40504-40510.

Uysal KT, Wiesbrock SM, Marino MW and Hotamisligil GS (1997) Protection from obesity-induced insulin resistance in mice lacking TNF-alpha function. *Nature* **389**:610-614.

Yoon JC, Puigserver P, Chen G, Donovan J, Wu Z, Rhee J, Adelmant G, Stafford J, Kahn CR, Granner DK, Newgard CB and Spiegelman BM (2001) Control of hepatic gluconeogenesis through the transcriptional coactivator PGC-1. *Nature* **413**:131-138.

Zeldin DC, Foley J, Boyle JE, Moomaw CR, Tomer KB, Parker C, Steenbergen C and Wu S (1997) Predominant expression of an arachidonate epoxygenase in islets of Langerhans cells in human and rat pancreas. *Endocrinol*ogy **138**:1338-1346.

Zhang CY, Baffy G, Perret P, Krauss S, Peroni O, Grujic D, Hagen T, Vidal-Puig AJ, Boss O, Kim YB, Zheng XX, Wheeler MB, Shulman GI, Chan CB and Lowell BB (2001) Uncoupling

protein-2 negatively regulates insulin secretion and is a major link between obesity, beta cell dysfunction, and type 2 diabetes. *Cell* **105**:745-755.

**Footnotes**

[*]This study was supported by the following National Institutes of Health grants: (HL-082733) to (M.H.W.); (ES-002710 and HL-059699) to (B.D.H.); and (HL-074167 and DK-44628) to (E.W. I.). B.D.H is a George and Judy Marcus Senior fellow of the American Asthma foundation.

[#]Reprint Requests: Mong-Heng Wang, Associate Professor, Medical College of Georgia, Augusta, GA 30912; E-mail: mwang@mcg.edu.

**Legends for Figures**

**Figure 1.** Genotyping and sEH tissue distribution. (A) Representative genotypic analysis of *Ephx2* (-/-) mice. Genomic DNA was isolated from mouse tails. The PCR products of *Ephx2* (-/-), *Ephx2* (+/-), and *Ephx2* (+/+) mice showed, respectively, a 160-bp band, 160- and 510-bp bands, and a 510-bp band. (B) Tissue distribution of sEH protein from *Ephx2* (+/+) and *Ephx2* (-/-) mice. Western blot analysis showed the expression of sEH protein in the kidney, liver, heart, spleen, lung, and islets of *Ephx2* (+/+) mice. In contrast, sEH protein expression was absent from the tissues in *Ephx2* (-/-) mice. Based on protein standards (Bio-Rad, Hercules, CA), the size of sEH protein is about 62 KDa. (C) Different concentrations of recombinant murine sEH (20-80 ng) and protein (40-160 μg) of *Ephx2* (+/+) islets for Western blot analysis. (D) Western blot of sEH in NIT-1 cells (50 μg protein) and mouse kidneys (3 μg protein).

**Figure 2.** Effects of sEH KO or inhibition on blood glucose levels in STZ mice. Weekly fasting blood glucose levels of *Ephx2* (+/+) + STZ (n = 10), *Ephx2* (-/-) + STZ (n = 11), *Ephx2* (+/+) + STZ + *t*-AUCB (10 mg/l in drinking water, n = 5), *Ephx2* (+/+) + vehicle (n = 5), and *Ephx2* (-/-) + vehicle (n = 5) after STZ treatment. $^{*}P < 0.05$ versus *Ephx2* (+/+) + vehicle; $^{\#}P < 0.05$ versus *Ephx2* (+/+) + STZ.

**Figure 3.** Glucose and insulin homeostasis in *Ephx2* (+/+) and *Ephx2* (-/-) mice treated with STZ. Intraperitoneal glucose tolerance test (IGTT) in STZ-induced diabetic mice. After a 6-h fast, mice were injected with 1 g/kg of glucose, i.p. (time = 0). (A) Blood glucose and (B) insulin were measured before and at varying time points after glucose administration. The

JPET Fast Forward. Published on May 3, 2010 as DOI: 10.1124/jpet.110.167544
This article has not been copyedited and formatted. The final version may differ from this version.



following mice were used: STZ-*Ephx2* (+/+) mice (n = 4) and STZ-*Ephx2* (-/-) mice (n = 4). $^{*}P < 0.05$ versus STZ-*Ephx2* (+/+).

**Figure 4.** Hyperglycemic clamp study in *Ephx2* (-/-) and *Ephx2* (+/+) mice. (A) Blood glucose levels (n = 6), (B) glucose infusion rate (n = 5), and (C) plasma insulin levels (n = 4) before and during hyperglycemic clamp. $^{*}P < 0.05$, $^{**}P < 0.01$ versus *Ephx2* (+/+).

**Figure 5.** (A) Intraperitoneal insulin tolerance tests (IITT) in *Ephx2* (+/+) and *Ephx2* (-/-) mice. After 6 h fast, mice (n = 4) from each group were injected with 1 U/kg of human insulin, i.p. (time = 0). Blood glucose concentrations were measured before and at 10, 30, and 60 min after insulin administration. (B) Fed (n = 5) and fasted (n = 4) glucagon levels in *Ephx2* (+/+) and *Ephx2* (-/-) mice. Glucagon levels in *Ephx2* (-/-) mice were indistinguishable from those of their littermate control, *Ephx2* (+/+) mice.

**Figure 6.** GSIS, ATP levels, and UCP2 expression in *Ephx2* (-/-) and *Ephx2* (+/+) islets. (A) *Epxh2* (+/+) and *Epxh2* (-/-) islets were treated with 3 mM glucose, 25 mM glucose, or 30 mM KCl plus 250 μM diazoxide plus 3mM glucose. Insulin concentrations in the media and islet pellets were determined using an insulin ELISA kit. The data shown are based on the results of five experiments. (B) Islets were isolated from *Epxh2* (+/+) mice incubated with either *t*-AUCB (100 μM) or vehicle for 12 h, then incubated with 3 mM glucose, 25 mM glucose, or 30 mM KCl plus 250 μM diazoxide plus 3 mM glucose. Insulin concentrations in the media and islet pellets were determined with an insulin ELISA kit. The data shown are based on the results of four experiments. (C) ATP levels. After overnight culture, *Ephx2* (-/-) or *Ephx2* (+/+) islets

were incubated with 3 or 25 mM glucose, then assessed for concentrations of ATP (n = 3). (D) Western blot analysis of UCP2 in *Ephx2* (-/-) and *Ephx2* (+/+) islets. $^{*}P < 0.05$, $^{**}P < 0.01$ versus *Ephx2* (+/+) incubated with vehicle.

**Figure 7.** Glucose-induced changes in intracellular calcium concentrations in *Ephx2* (-/-) and *Ephx2* (+/+) cells. (A) Representative $Ca^{2+}$ traces obtained from individual *Ephx2* (-/-) (n = 19) and *Ephx2* (+/+) (n = 16) islet cells in response to 3 mM glucose, 25 mM glucose, or 30 mM KCl plus 250 μM diazoxide plus 3 mM glucose. (B) Quantitative summary of the intracellular calcium concentration response to different stimulators. $^{**}P < 0.01$ versus *Ephx2* (+/+) mice. Cells representing at least 5 different mice from each genotype were analyzed.

**Figure 8.** (A) In *Ephx2* (-/-) mice treated with vehicle, pancreases showed no apoptotic cell. In *Ephx2* (+/+) mice treated with vehicle, pancreases showed no apoptotic cell. On day 14 after STZ treatment, representative pancreatic photomicrography showed 2 apoptotic cells in islet of *Ephx2* (-/-) mice. On day 14 after STZ treatment, representative pancreatic photomicrography showed 6 apoptotic cells in islet of *Ephx2* (+/+) mice. (B) Quantification analysis of TUNEL staining showed that islet cell apoptosis in the STZ-*Ephx2* (+/+) group is significant higher than does the STZ-*Ephx2* (-/-) group. n = 4. $^{*}P < 0.05$ versus STZ-*Ephx2* (+/+) mice.

JPET Fast Forward. Published on May 3, 2010 as DOI: 10.1124/jpet.110.167544
This article has not been copyedited and formatted. The final version may differ from this version.

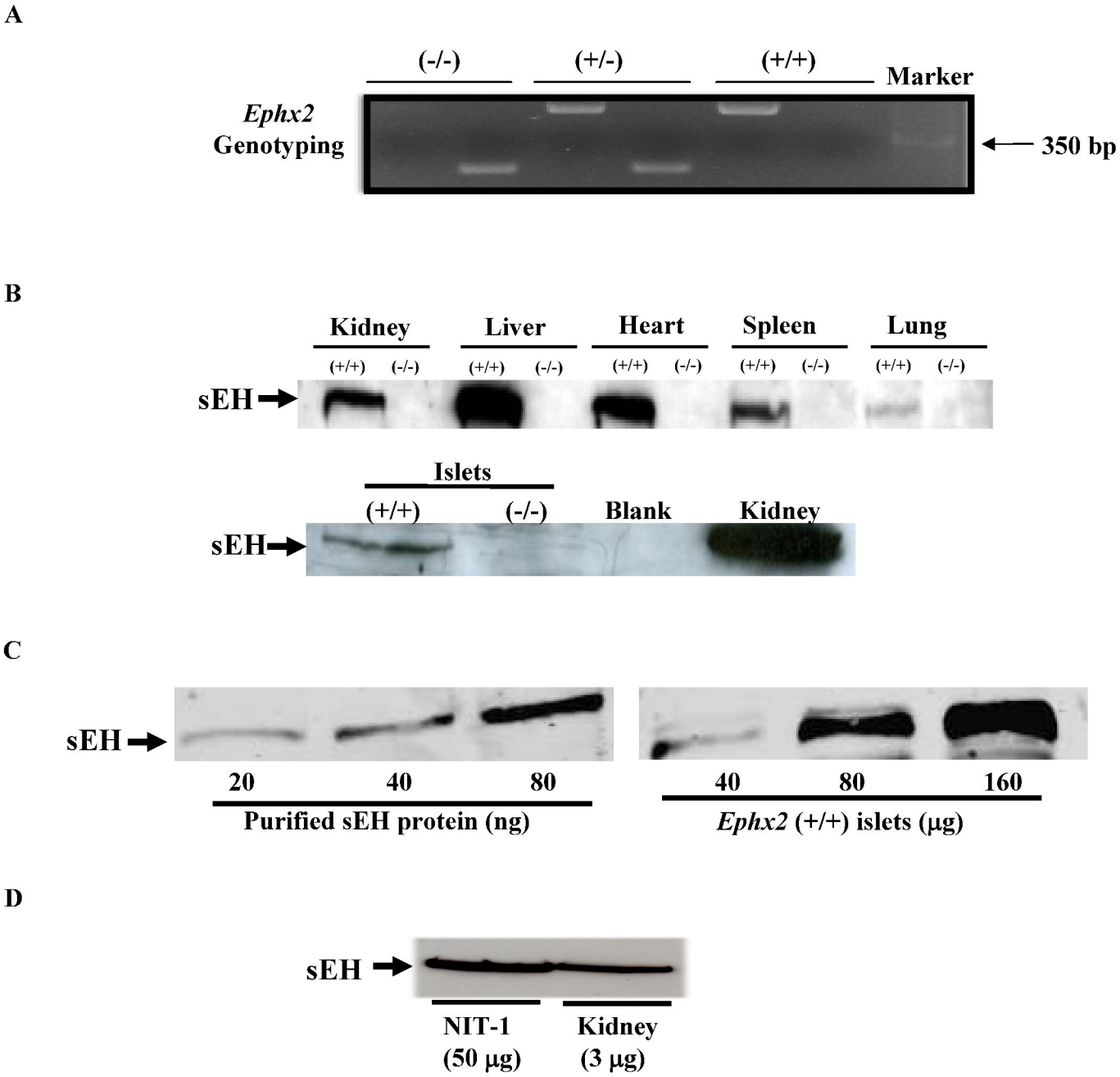


Fig. 1

JPET Fast Forward. Published on May 3, 2010 as DOI: 10.1124/jpet.110.167544
This article has not been copyedited and formatted. The final version may differ from this version.

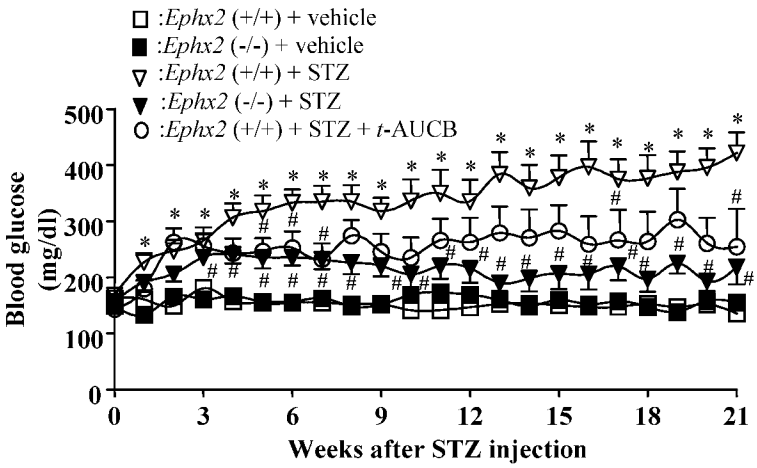


**Fig. 2**

JPET Fast Forward. Published on May 3, 2010 as DOI: 10.1124/jpet.110.167544
This article has not been copyedited and formatted. The final version may differ from this version.

A

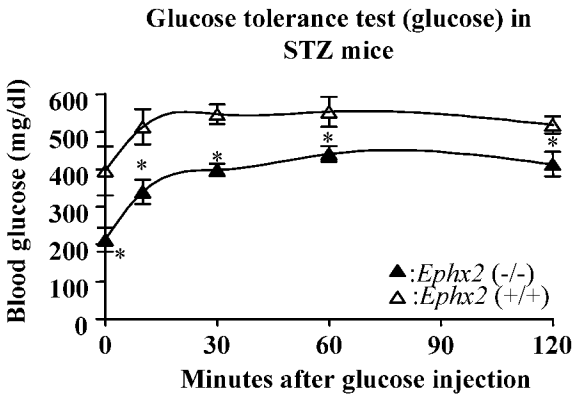


B

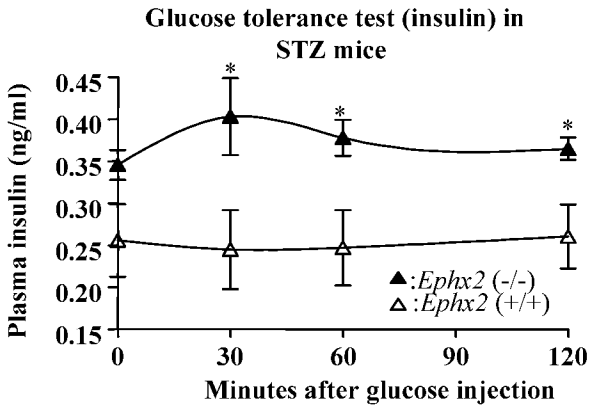


**Fig. 3**

JPET Fast Forward. Published on May 3, 2010 as DOI: 10.1124/jpet.110.167544
This article has not been copyedited and formatted. The final version may differ from this version.

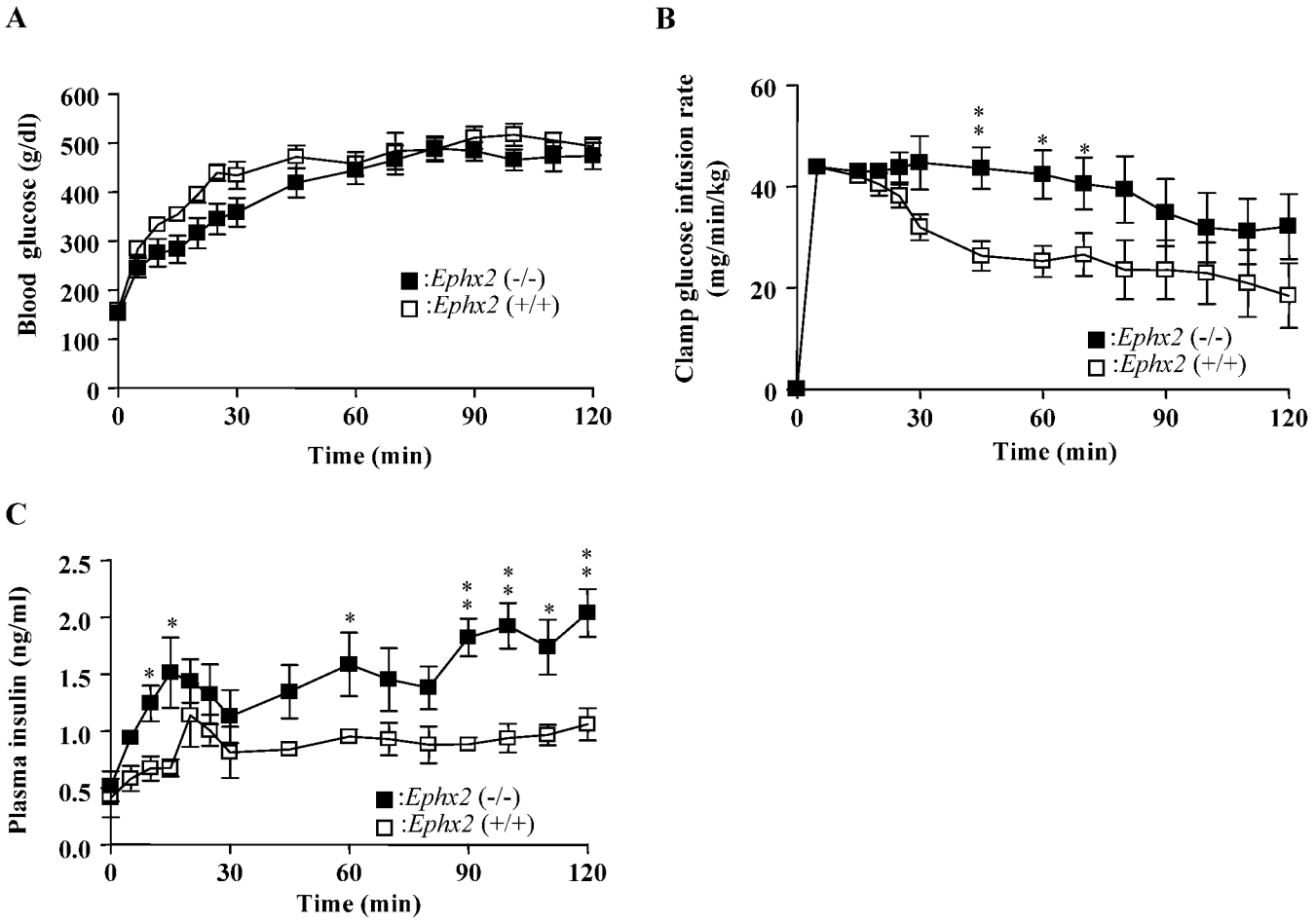


**Fig. 4**

JPET Fast Forward. Published on May 3, 2010 as DOI: 10.1124/jpet.110.167544
This article has not been copyedited and formatted. The final version may differ from this version.

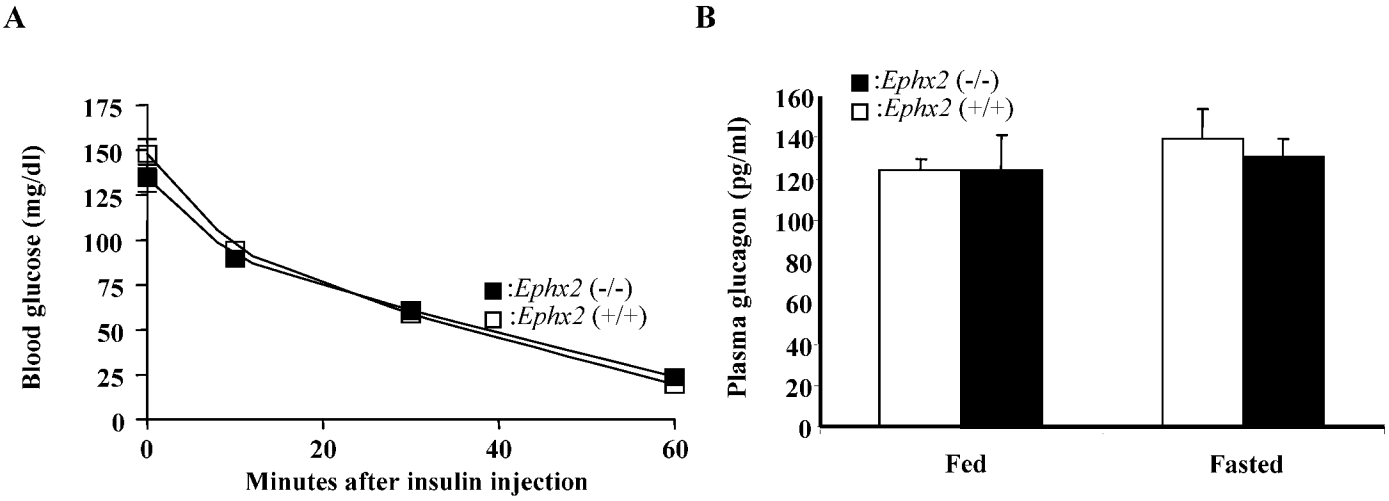


**Fig. 5**

JPET Fast Forward. Published on May 3, 2010 as DOI: 10.1124/jpet.110.167544
This article has not been copyedited and formatted. The final version may differ from this version.

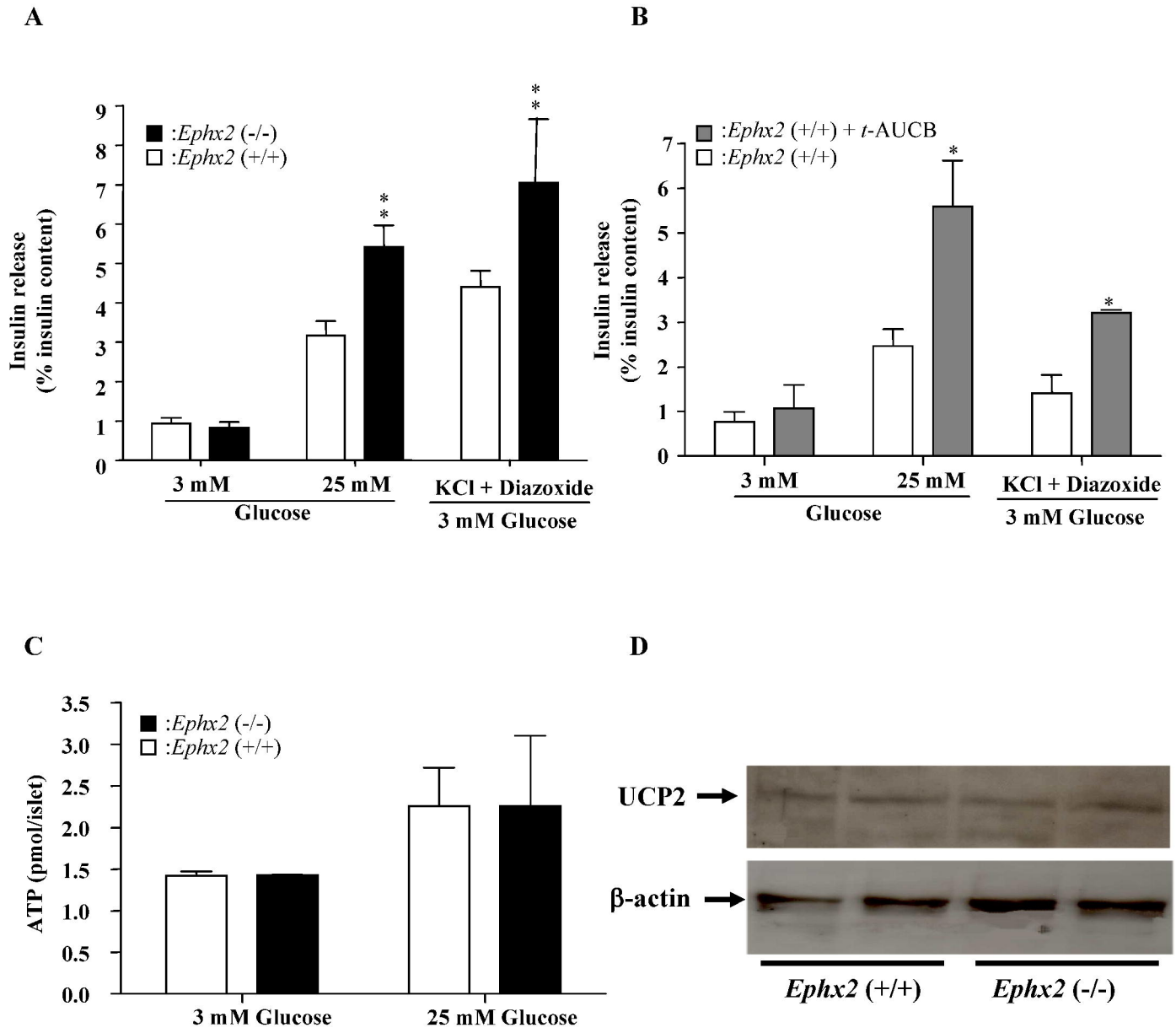


**Fig. 6**

JPET Fast Forward. Published on May 3, 2010 as DOI: 10.1124/jpet.110.167544
This article has not been copyedited and formatted. The final version may differ from this version.

A

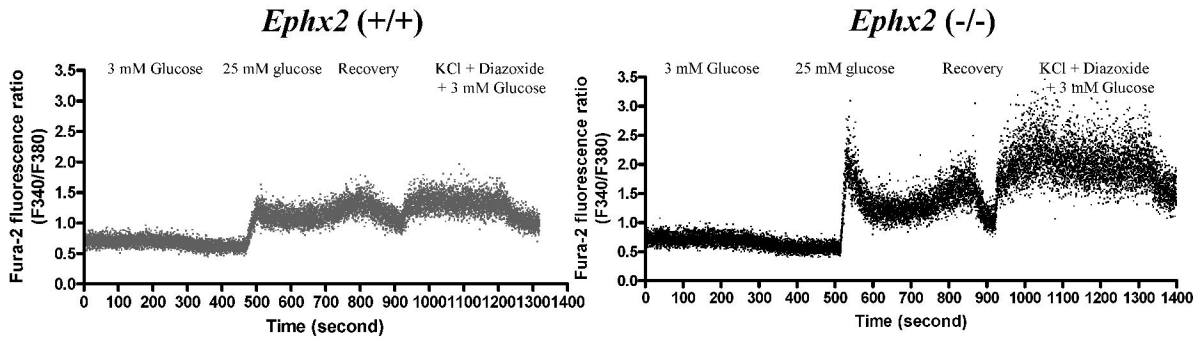


B

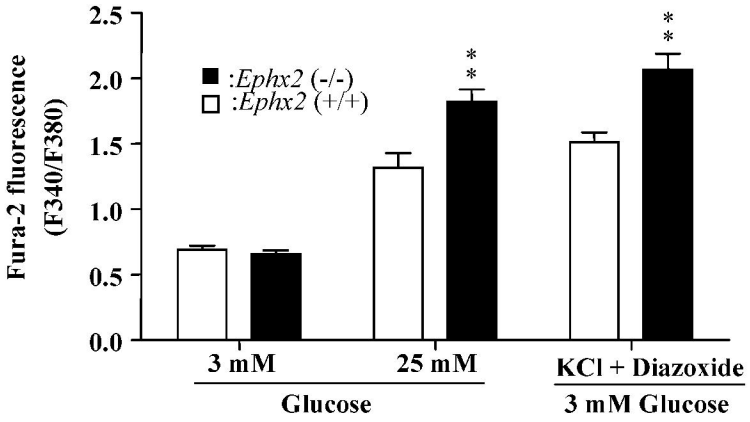


Fig. 7

JPET Fast Forward. Published on May 3, 2010 as DOI: 10.1124/jpet.110.167544
This article has not been copyedited and formatted. The final version may differ from this version.

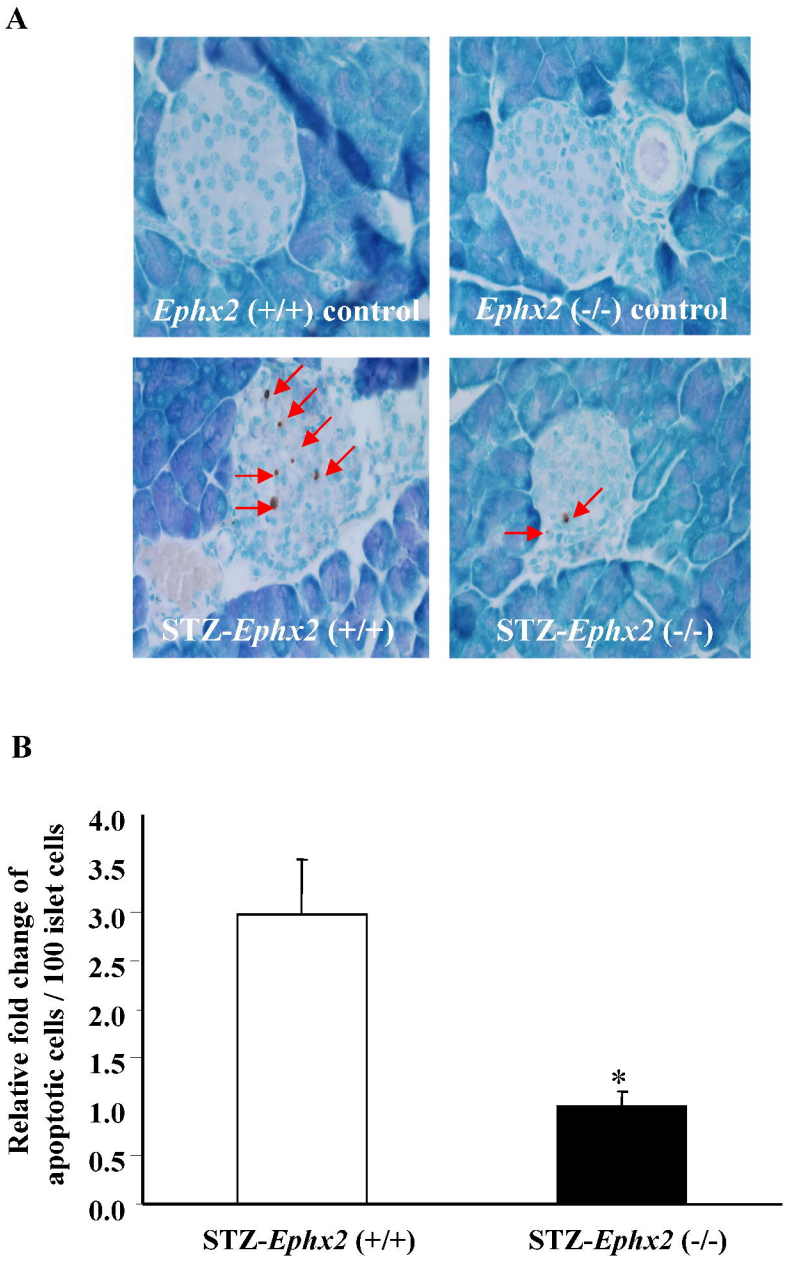


**Fig. 8**